

CSP-reference power plant “Made in Germany”

Cite as: AIP Conference Proceedings **2445**, 050003 (2022); <https://doi.org/10.1063/5.0085877>
Published Online: 12 May 2022

Jürgen Dersch, Matthias Binder, Cathy Frantz, et al.



View Online



Export Citation

ARTICLES YOU MAY BE INTERESTED IN

[Preface: SolarPACES 2020 - 26th International Conference on Concentrating Solar Power and Chemical Energy Systems](#)

AIP Conference Proceedings **2445**, 010001 (2022); <https://doi.org/10.1063/12.0009334>

Lock-in Amplifiers up to 600 MHz



Zurich
Instruments



CSP-Reference Power Plant “Made in Germany”

Jürgen Dersch^{1,a)}, Matthias Binder^{2,b)}, Cathy Frantz^{3,c)}, Stefano Giuliano^{3,d)},
Fabian Gross^{4,e)}, Holger Hasselbach^{5,f)}, Nadine Kaczmarkiewicz^{2,g)},
Freerk Klasing^{6,h)}, Jaime Paucar^{7,i)}, Thomas Polklas^{8,j)},
Christian Schuhbauer^{2,k)}, Axel Schweitzer^{4,l)}, Alexander Stryk^{5,m)}, and
Dennis Többen^{8,n)}

¹*DLR Institute of Solar Research, Linder Höhe, 51147 Köln, Germany*

²*MAN Energy Solutions SE, Werftstrasse 17, 94469 Deggendorf, Germany*

³*DLR, Institute of Solar Research, Pfaffenwaldring 38-40, 70569 Stuttgart, Germany*

⁴*sbp sonne GmbH, Schwabstraße 43, 70197 Stuttgart, Germany*

⁵*Tractebel Engineering GmbH, Friedberger Straße 173, 61118 Bad Vilbel, Germany*

⁶*DLR, Institute of Engineering Thermodynamics, Linder Höhe, 51147 Köln, Germany*

⁷*Steinmüller Engineering GmbH, Fabrikstraße 5, 51643 Gummersbach, Germany*

⁸*MAN Energy Solutions SE, Steinbrinkstr. 1, 46145 Oberhausen, Germany*

^{a)}Corresponding author: juergen.dersch@dlr.de

^{b)}matthias.binder@man-es.com

^{c)}cathy.frantz@dlr.de

^{d)}stefano.giuliano@dlr.de

^{e)}f.gross@sbp.de

^{f)}holger.hasselbach@tractebel.engie.com

^{g)}nadine.kaczmarkiewicz@man-es.com

^{h)}freerk.klasing@dlr.de

ⁱ⁾jaime.paucar@steinmueller.com

^{j)}thomas.polklas@man-es.com

^{k)}christian.schuhbauer@man-es.com

^{l)}a.schweitzer@sbp.de

^{m)}alexander.stryk@tractebel.engie.com

ⁿ⁾dennis.toebben@man-es.com

Abstract. A reference solar tower power plant with molten salt as heat transfer and storage medium has been designed. In addition to the general layout of this plant, the paper contains selected details about component sizing and optimization. The final layout and optimization of the least cost storage capacity for 2 different operating schemes has been checked by an annual yield calculation for an exemplary site in Morocco.

INTRODUCTION

Today CSP plants are tailor-made installations requiring a lot of engineering work for optimization and site adaption. This paper gives an overview about the results of the German national research project “CSP-Reference Power Plant”. The major goal of the project consortium from German industry supplemented by DLR is to develop and optimize a solar tower plant with 2-tank molten salt thermal storage and publish a blueprint which can be used as starting point for future CSP power plants. This might be used to save costs and time for future plants.

Figure 1 shows the overall system as well as the major components and the responsible companies for these components. As further partners Tractebel Engie and DLR are involved with more general tasks and therefore not shown in Fig. 1.

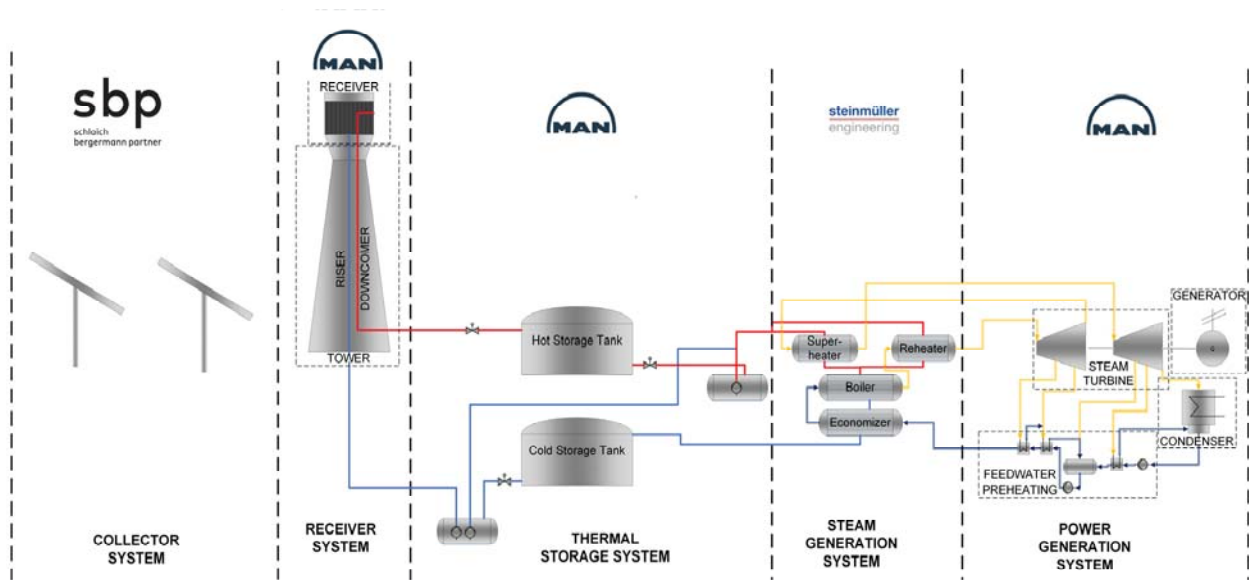


FIGURE 1. Subsystems of a molten salt solar tower plant and responsibility of the involved companies

METHODOLOGY

In a first step recent CSP projects have been analyzed to find typical requirements which may be important for future plants. Nominal electrical output is typically between 100 and 200 MW_e, with some smaller units in regions where the technology is being introduced for the first time. In principle there are a large number of degrees of freedom for the design of a solar tower power plant and a full enumeration and optimizing process could be very time consuming. Therefore the approach was different: starting from the idea that each industrial partner knows very well the specific costs of his individual subsystem, a preliminary design of the plant was made by using these least cost subsystems. This was particularly valid for the heliostat field and the power block unit.

sbp sonne GmbH found, that a heliostat field made of its Stellio [1] units of about 1.5 km² of aperture area would lead to minimal specific costs for good DNI and clear atmosphere conditions. For smaller solar fields the fixed cost components like engineering, assembly hall, optical quality checking system etc. and for larger fields the decreasing efficiency of the outmost heliostats are raising the specific costs. Similar MAN Energy Solutions SE found that their largest turbine units capable for fast daily start/stop operation would show lowest specific investment costs. These turbines have a gross electricity output of about 200 MW. From some simplified first simulation runs, the project consortium found that the matching receiver thermal power would be 700 MW_{th} and the storage size should be in the range of 12 full load hours to operate the turbine between sunset and sunrise. For the molten salt thermal storage, we found that specific costs are decreasing with increasing storage capacity. Technical limits for single tanks require the step from 2 tanks to 4, 6, etc. if a certain size is exceeded with a step up in specific costs. This step is not as big, that it would limit the storage capacity of our plant.

This starting configuration was fixed and the subsystems solar field, receiver, storage, steam generator and power block were optimized separately, of course taking into account the interfaces to other subsystems and their interdependency where applicable. The involved companies with their special expertise in different areas ensure the market availability of the subsystems. An annual yield calculation was finally used for fine tuning and LCOE optimization.

BOUNDARY CONDITIONS

Most of the CSP plants, which are currently under development are combined with PV plants to make use of the benefits of cheap direct solar electricity production from PV paired with cheap thermal storage and dispatch-able solar electricity production from CSP. Therefore the major role of the CSP plants will be rather to produce electricity when the sun is not shining. Recent projects enforce this behavior by defining appropriate tariff structures or by requiring a certain fraction of solar electricity production after sunset. Two operating scenarios which can be considered as “typical” have been found: either operation from sunset to sunrise (called “**Night time operation**” in this paper) or operation for several hours (about 5-7 hours) after sunset (called “**Peaker operation**”).

Although the CSP-Reference plant shall be adaptable to many sites, the study requires an example site to conduct optimization and annual yield calculations. Morocco’s Ouarzazate has been chosen as exemplary site since it is located in a region providing good conditions for solar electricity generation, is at a moderate latitude (31°N), and shows good but not outstanding irradiation. We have used a typical meteorological year dataset generated by METEONORM software [2] with annual sums of 2518 kWh/m² for DNI and 2123 kWh/m² for GHI.

The power block of the CSP plant is allowed to start at about sunset (considering different starting times for each season) but not during daylight hours. After startup it shall operate at full load, which means that the net electricity which can be delivered to the grid is almost constant until the thermal storage runs empty. There is some impact of ambient conditions on the net electrical output, particularly when one compares summer and winter, but this difference is in the range of ±2 % and thus can be neglected in the context of this study.

HELIOSTAT FIELD AND SOLAR RECEIVER

These components need to be designed and optimized jointly in order to come to an efficient and durable system. Nine different variants for a 700 MW_{th} receiver are designed on a thermo-hydraulic basis. These receiver-designs show mean flux densities varying between 400 and 600 kW/m². They are aimed at either optimizing costs or optimizing efficiency. This is either achieved by reducing overall absorber size and the number of welds or by increasing the flow velocity inside the absorber tubes. The receiver efficiency as a function of load and wind velocity of each variant is computed using an analytical receiver model. In this model local salt temperatures are computed for each panel based on a local energy balance of each axial element. The model considers absorbed solar radiation, forced convective heat transfer to the salt based on Nusselt-correlations [3], IR losses to ambient and convection losses to ambient. [3] The model was validated by a detailed thermal FEM model [4]. Furthermore, the pressure drop, and hence the required pumping power was estimated [4]. For each receiver variant a cost estimation was made. Based on this data the thermo-optical annual efficiency and LCOH of the variants is simulated. Out of the 9 thermo-hydraulic configurations, three designs were selected to be integrated in the thermo-optical simulation of heliostat field and receiver.

The task for the heliostat field is the supply of power to the receiver whilst adhering to the flux density limits of the absorber. For this supply to be cost efficient, both the field and receiver cost and efficiencies need to be balanced. The large scale heliostat field (1.5 km² being 14 % larger than Noor III) allows to reduce the specific cost more than the increase in attenuation loss at a good site. The receiver variants discussed above have relatively low flux density limits on the final hot panels in the south, already pushing heliostats to positions further north to be able to irradiate subcritical surfaces. The in-house tool sbpRAY [6] assesses the annual efficiencies (cosine, shading, tower shading, blocking, attenuation, intercept) of fields with the three receiver geometries (large ~ 0.4 MW/m², medium ~ 0.5 MW/m², small ~ 0.6 MW/m² average flux density in full load) positioned at heights of 200, 225, 250 and 275 m above ground.

The results show that the higher intercept for the larger receiver is compensated by lower thermal efficiencies such that the overall efficiency is very similar. Therefore, the consortium chooses the receiver variant with the most favorable material and manufacturing options.

The analysis of tower heights shows that the field efficiencies improve with higher towers, but the assumed cost of construction and running costs for the salt pumps and assumed free land make the smallest tower techno-economic most attractive in terms of levelized cost of heat (LCoH). It also comes with the lowest risk (Fig. 2).

The annual performance of the 1.5 km² of mirror area (30927 Stellio heliostats) in hourly resolution shows balanced losses due to power below and above receiver cutoff due to initially assumed limits of 30 % - 100 % for the operational range. The heliostat field area fits to the proposed receiver in the meteorological conditions in Ouarzazate, Morocco.

The subsequent analysis showed, that a different choice of salt pumps and detailed analysis of the flux distribution on the receiver in overload situations allows extending the operational range to 15 % - 110 % of the 700 MW_{th}. The gained production reduces the LCoH by 7 %.

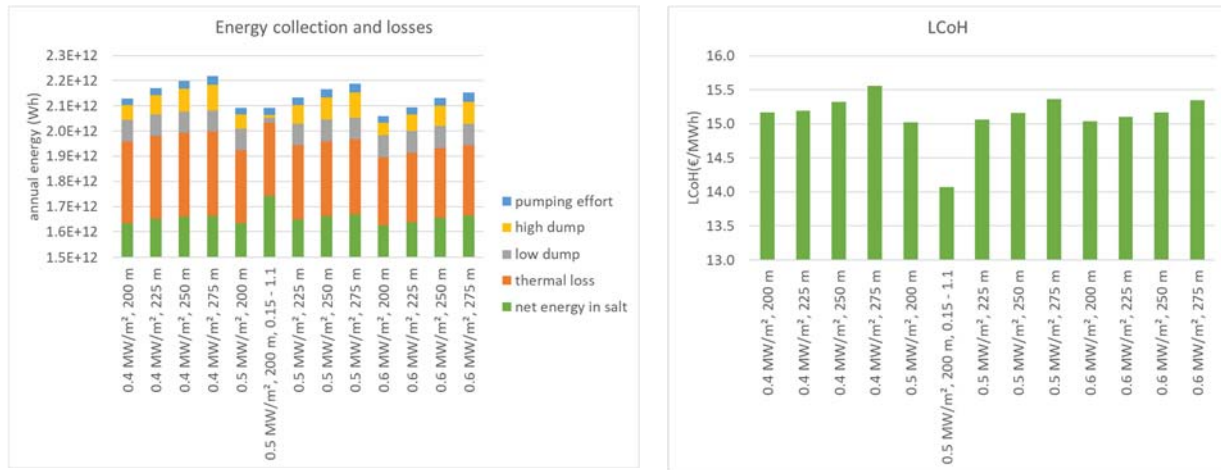


FIGURE 2. Annual energy output (left) and levelized cost of heat at receiver entrance (right) for different mean flux densities and different tower heights

Based on the optimized field layout a final receiver design is deduced by techno-economic evaluation. For this evaluation points like material demand and availability, pressure loss, construction effort, durability, lifetime and road transport were taken into account. Austenitic materials are chosen for the receiver, because of their low costs compared to nickel-based alloys. The receiver is subdivided in a number of components suitable for road transport. The panels are for example divided into two parts just for better handling. TABLE 1 provides an overview of some important key features and Fig. 3 gives an impression of the intended panel configuration.

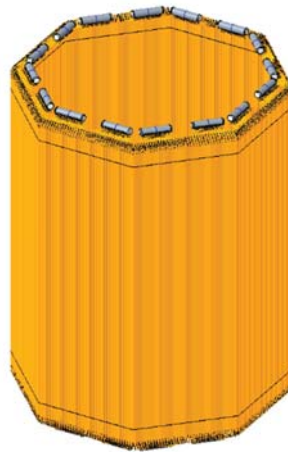


FIGURE 3. Panel configuration of the receiver

The mean flux density of the receiver results from the lifetime evaluation. This evaluation is done by an analytical approach based on the procedure proposed by Smith [5]. The calculations are based on the load collective method proposed by Kistler et al. [8]. The load collective was deduced using a rainflow algorithm based on weather data of the location Morocco. Local allowable flux density limits are determined for the receiver based on lifetime consumption due to fatigue damage. The results of this analysis are shown in Fig. 4.

The mean flux density can be obtained by applying a reduction factor. A validation of this analytical approach is done by Finite-Element-Method (FEM) with a simplified receiver model. For this approach a sophisticated material model is implemented and thermal loads are applied. The evaluation is done by the creep-fatigue evaluation presented

in ASME Section III Subsection HBB Appendix T with one modification. The FEM results differ from the analytically calculated lifetime in a manageable manner. Before launch some more detailed simulations have to be done.

TABLE 1. Key features of receiver

Parameter	Value
Mean flux density [kW/m ²]	536
Mean flow velocity [m/s]	3.36
Ratio height/diameter [-]	1.21
Number of panels [-]	8
Irradiated tube length [m]	22.8
Panel width [m]	7.2
Minimal part load [%]	19

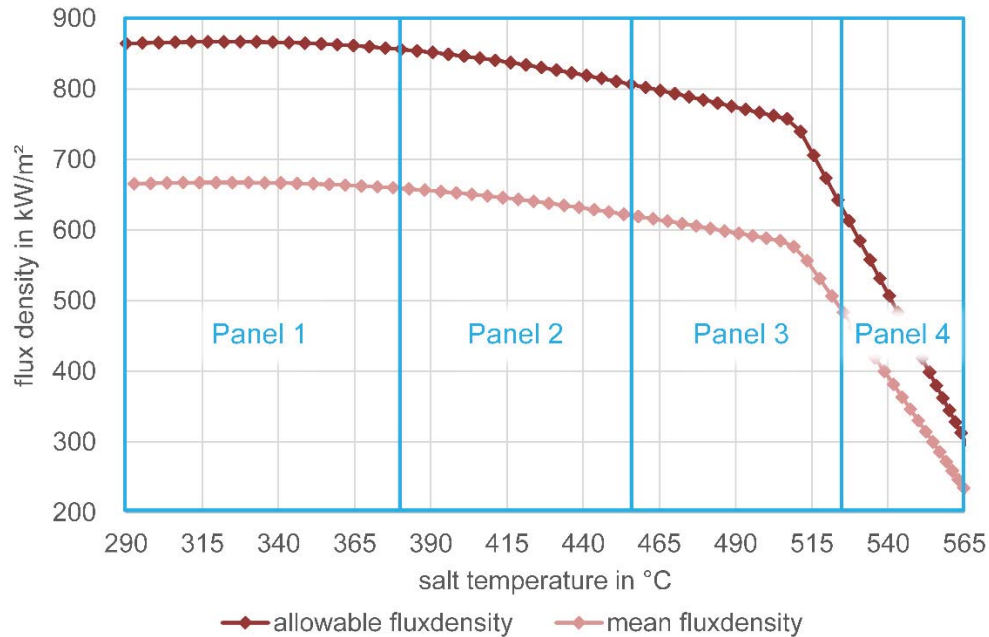


FIGURE 4. Allowable flux density over flow path

MOLTEN SALT CYCLE AND ENERGY STORAGE

The molten salt cycle consists of a 2-tank system built out of one cold and two hot storage tanks to handle thermal expansion. The cold salt pumps, which are placed in the cold storage tank, are feeding the solar receiver via the inlet vessel. To ensure a good part load behavior – below 20 % – the cold salt tank is equipped with five pumps. The inlet vessel has the task of providing the receiver with sufficient salt. The control valve in the receiver feed line, which is responsible for controlling the salt outlet temperature, has to react fast due to changes of solar heat input. To generate stable conditions the inlet tank is pressurized. Furthermore this vessel feeds an emergency flushing. After passing the solar receiver the salt enters the outlet vessel. The volume of the outlet vessel is determined by the emergency flushing time and the resulting mass flow rate. After passing the outlet vessel the salt enters the hot storage tank. The hot storage tank is equipped with four salt pumps in case of the night time operation and six pumps in case of peaker operation. The hot salt pumps feed the steam generator system and by cooling down the molten salt the live steam is produced.

The operating concept of the molten salt cycle is divided into the following modes:

- Standby mode (solar tower off)
- Night mode (salt circuit standby)
- Receiver start-up (solar tower standby and heliostat field standby)
- Load operation (solar operation)

During a long-term shut down, e.g. due to maintenance work or a weather forecast with hardly any direct normal irradiance (DNI), the solar tower including the heliostat field is shut down. To collect solar energy the following steps have to be absolved. The salt circuit is preheated up to 290 °C and then the cold pumps are started to fill the riser and downcomer. When the set point in the inlet vessel is reached, valve positions are changed so that the flow direction in the downcomer turns and corresponds to operation mode. Cold salt is pumped through the riser, receiver bypass and downcomer back to the cold storage tank. Meanwhile some heliostats are focusing and preheating the receiver. After both parts are in standby mode, the receiver is prepared for starting. The inlet vessel is pressurized and valves are opened to flood headers and absorber tubes. Then the serpentine flow is established by closing venting and draining valves. Salt flows through absorber tubes and solar operation can be started by increasing the flux density on the receiver. All operating states with possible transitions are shown in Fig. 5.

The flux density is reduced to shut down the receiver, either by moving the heliostats to the standby or stow position or by the available DNI based on the time of day. Some heliostats are still needed to prevent rapid cooling of the receiver. In the next step the receiver is drained and all heliostats can move to their stow position. Then the salt flow is directed through the receiver bypass which is reduced to a minimum at night mode. If the salt circuit has to be drained too, the entire solar tower is switched off.

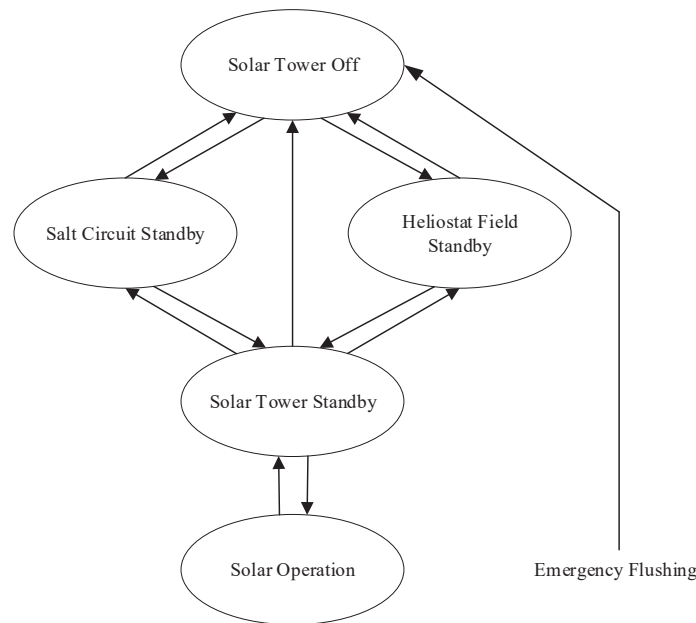


FIGURE 5. Overview of receiver operating states

In case of e.g. a station black out the emergency flushing is triggered and the valves changes to their safety position. At the same time the heliostats get the command to change into stow position. The flux density will be reduced immediately. Cold salt flows out of the inlet vessel through the receiver. The driving force for this flow is the constant pressure in the inlet vessel, which is maintained by the emergency vessel as reservoir. After 30 seconds, the emergency flushing stops and the receiver valves are opened to drain the receiver and shut down the solar tower. The emergency flushing can start at any time - in any state and transition.

Solar salt can be heated up to a temperature of 565 °C with low decomposition - and even higher temperatures are possible by carefully controlling the salt chemistry. Although the eutectic (Solar Salt 45) has the lowest melting point, KNO₃ is the more cost-intensive component, which increases the investment costs accordingly.

The chemical reaction system of nitrate melts is very complex. The decomposition of the sodium nitrates produces oxides, which lead to corrosion. To counteract the decomposition of the salt components and reduce the corrosion rates, the salt storage tanks could be designed as closed system and superimposed with technical air. In a closed system the decomposition of the salt runs into a thermodynamic equilibrium and comes to a standstill. Nevertheless, such a closed system is not state of the art and still under development.

For the cold tank an alloyed heat-resistant steel SA 204 Gr B is being considered. The stainless austenitic steel 316Ti is considered for the hot tank. This material has shown almost no chromate formation in isothermal investigations at 560 °C by DLR [9]. Since the material 316Ti is a common steel, the additional costs are low compared to 321, for example. Also the materials 321H and 347H are good alternatives for the hot storage tank.

The storage tanks are insulated with rock wool mats. A distinction is made between the insulation of the hot and cold tanks. The hot tank is insulated with an insulation thickness of about 500 mm, whereas the insulation thickness of the cold tank is reduced to 350 mm.

The structure of the foundation is shown in TABLE 2. The foundation also contains the insulation to the ground. Due to the higher temperature in the hot tank the upper layer needs to be made of bricks to withstand the thermal load.

TABLE 2. Storage Foundations

	Hot Tank	Cold Tank
Brick	250 mm	0 mm
Foamglass	400 mm	500 mm
Concrete	50 mm	50 mm
Compacted gravel	150 mm	150 mm
Sand	300 mm	300 mm

One main cost driver of the salt storage system is the solar salt itself. Currently, the costs for the salt are assumed to be in a range between 8.5 and 10 USD/kWh_{th}. A price of 1.6 USD/kWh_{th} for the one-time melting process has to be considered. For the overall storage tank system including the heater, balance of plant, transport and mark-up the price is in a range between 24 USD/kWh_{th} and 26 USD/kWh_{th}. An additional air system to pressurize the tank to prevent decomposition of the salt will increase the costs. At the actual state of the project the costs for a closed system are not included.

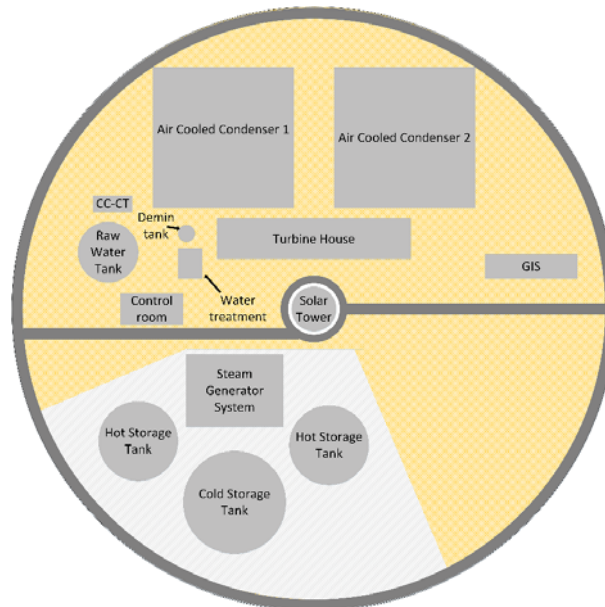


FIGURE 6. Plant layout in the center of the heliostat field for peaker operation 2 x 200 MWel

The available salt pumps determine the maximum height of the storage tanks. Their shaft is limited to 22 m so that the tank height should not exceed 21 m. This results in a diameter of around 45 m for the cold storage tank and around 35 m for the two hot storage tanks. Figure 6 shows the plant layout for the peaker option with $2 \times 200 \text{ MW}_{el}$.

STEAM GENERATOR AND POWER CYCLE

These are again 2 components which can only be optimized together since they are closely coupled and separate optimization would most probably not result in an optimized combination. Although the first approach was to use an once-through steam generator, due to the faster load changing capabilities, the findings for the typical operation scheme defined by the boundary conditions did change this choice. Since the CSP power plant is expected to run at constant load close to its nominal power, a natural convection steam generator will be more economic. It shows lower specific investment costs as well as lower pressure loss for the water/steam side.

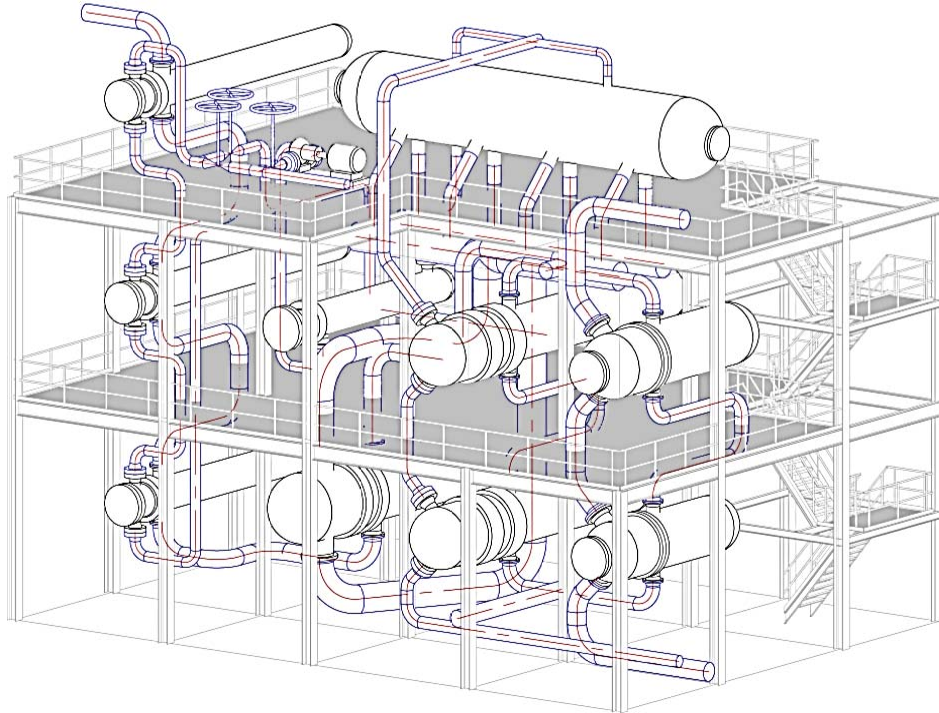


FIGURE 7. Steam generator arrangement

The schematic power block design is shown in Fig. 8 with MAN MST080 and MST120 steam turbines as major components. The power block is designed as single reheat cycle with 140 bar/550°C live steam conditions, since the increase in performance due to double reheat configuration does not justify the additional costs.

The system is equipped with an air cooled condenser since CSP plants will typically be installed in regions where water is scarce. In order to prevent salt freezing especially during start-up procedure, the last high pressure feed water pre-heater can be fed either by a sliding bleed at the high pressure steam turbine or by live steam.

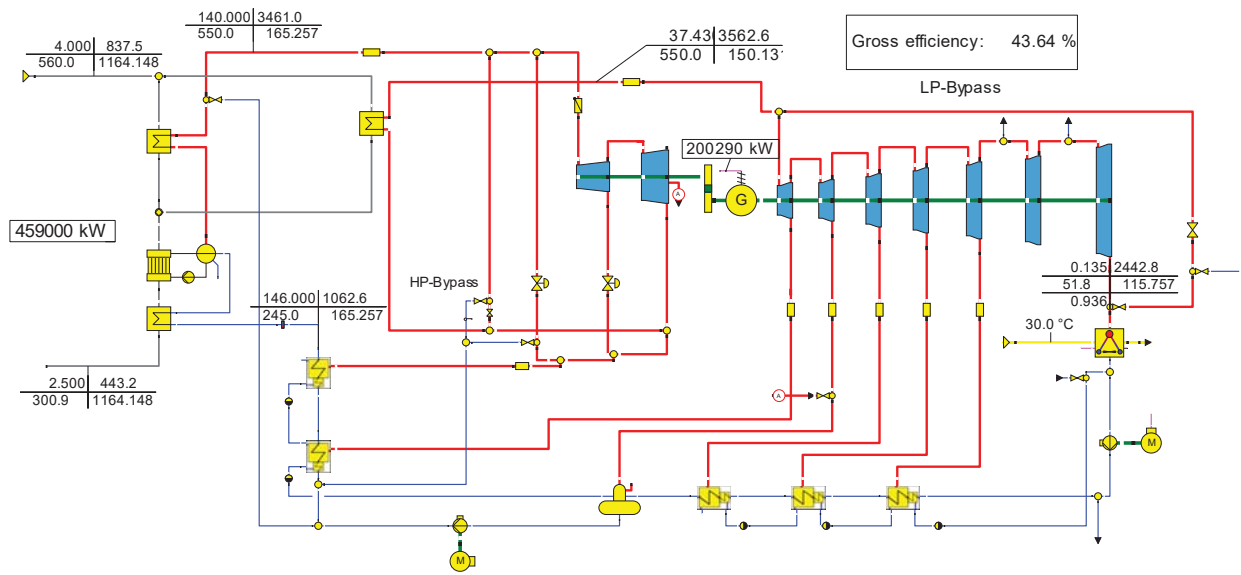


FIGURE 8. Heat balance diagram of the power cycle

OVERALL SYSTEM AND ANNUAL YIELD

Finally the optimized subsystems and their performance were used to find the storage capacity which would lead to the lowest LCOE. For this purpose the specific costs of the subsystems must be compiled and used together with performance data and the typical meteorological dataset. The annual yield calculation was done with the DLR software tool greenius [10]. In addition to the 2 operation schemes mentioned above (night time and peaker), the solar only operation was also simulated. Although this would probably not be considered as relevant operating scheme for future CSP plants, it is the operation scheme which leads to the smallest thermal storage and the largest number of operating hours and has been calculated as reference for LCOE. “Solar only” operation means, the plant may produce electricity whenever possible and the first priority is to run the power block. Only when the power block runs at full load, excess solar heat from the receiver is stored and used during times with less heat from the solar field. In contrast in the night time and peaker operating schemes the power block is not operated during daylight hours, but they are just used to collect solar heat and charge the thermal storage. All plants are using identical solar field, receiver and power block design. The peaker CSP plant has 2 of the 200 MWe power blocks instead of one for the night time operation plant. This modular approach helps also to reduce costs.

Figure 9 shows the operation of the CSP plant during 4 sunny days throughout the year. The blue line represents DNI times aperture area, thus the solar resource the system could use. Receiver heat output is shown as red line which is of course lower than the solar resource due to the efficiency of the system. There is also a time delay of the receiver heat output compared to the solar resource representing the startup of the molten salt and the receiver. The green line shows net electricity production starting after sunset and lasting until sunrise next morning, or until the storage is empty. The orange line shows heat which could be produced by the solar field/receiver system but which cannot be used since the storage is fully charged and the power block is not running (dumping). As known from other studies, the least cost system layout will show some “dumped heat, particularly during summer, since otherwise the thermal storage would not be utilized in an economic way.

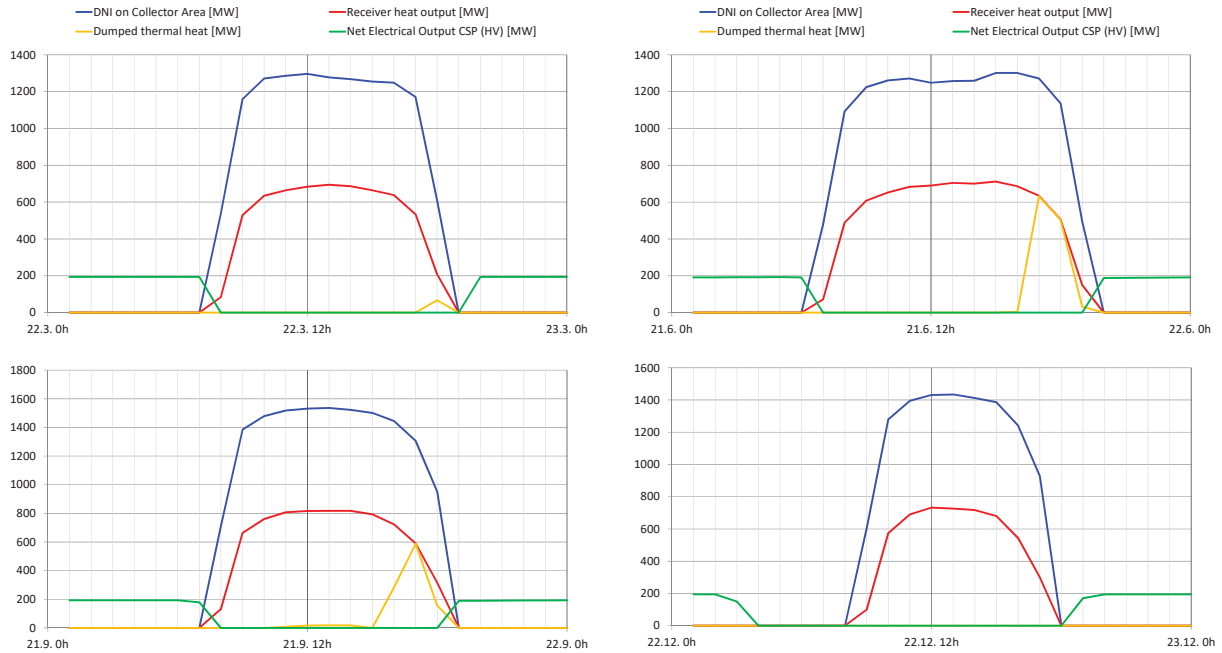


FIGURE 9. Operation of the CSP plant with 13 h storage capacity on typical days (Night time operation mode)

In TABLE 3 the LCOE optimized systems are shown as well as their relative LCOE. The absolute numbers are not shown here since the final cost estimation is not yet completed but the authors do not expect any large changes, especially not for the relative values. As mentioned above, the CSP plant operated in solar only mode gives the least LCOE and would have a thermal storage with 5 hours of full load capacity. The plant designed for night time operation should have 13 hours of thermal storage and the LCOE is increased by about 30% compared to the solar only plant.

The peaker plant should have a 6 hours thermal storage thus somewhat smaller than the night time operation plant but as TABLE 3 shows, using the same thermal storage capacity in MWh, would increase the LCOE only in a negligible way. Thus the storage capacity in MWh for both systems may be chosen identically, thus saving further engineering costs.

TABLE 3. Results of the annual yield calculation to find the cost optimal storage capacity

Operation mode	Nominal power [MW]	Storage Capacity [h]	Storage Capacity [MWh]	Rel. LCOE	Net electricity [GWh]	Solar capacity factor ^{*)}
Solar only	200	5	2295	1.00	672.4	41
Night time	200	13	5967	1.30	628.8	69
Peaker	2×200	6	5508	1.84	539.5	64
Peaker	2×200	6.5	5967	1.85	544.9	64

CONCLUSIONS

A reference molten salt solar tower plant has been defined for ~12 h night time and ~6 h peaker operation scenarios. These configurations are important to complement photovoltaic plants for future projects. Cost savings are due to standardized and modular design and the utilization of cost optimized subsystems. Cost optimization here is made for the systems of the involved companies but the authors expect that similar rules should be valid also for other suppliers.

This plant design should fit also to other sites. Of course some fine tuning during detailed engineering phase will be required. The full results of the project and more details about the systems will be summarized and published by the end of this year

ACKNOWLEDGMENTS

The authors want to acknowledge financial support by the German Federal Ministry for Economic Affairs and Energy (Reference number: 0324253). The sole responsibility for the contents lies with the authors.

REFERENCES

1. Markus Balz, V. Göcke, Thomas Keck, F. von Reeken, Gerhard Weinrebe, Markus Wöhrbach, "Stellio - development, construction and testing of a smart heliostat," in *SolarPACES Annual Conference 2015*, Cape Town, South Africa.
2. <https://meteonorm.com/en/>
3. VDI Wärmeatlas 10. Auflage 2006.
4. R. Uhlig et al., "Effects of vertically ribbed surface roughness on the forced convective heat losses in central receiver systems," *AIP Conference Proceedings* 1734, p. 030036 (2016).
5. C. Frantz et al., "ASTRID© – Advanced Solar Tubular Receiver Design: A powerful tool for receiver design and optimization," *AIP Conference Proceedings* 1850, p. 030017 (2017).
6. Daniel Gebreiter, Gerhard Weinrebe, Markus Wöhrbach, Florian Arbes, Fabian Gross, Willem Landman, "sbpRAY – A fast and versatile tool for the simulation of large scale CSP plants," *AIP Conference Proceedings* 2126, p. 170004 (2019); <https://doi.org/10.1063/1.5117674>.
7. D. C. Smith, "Design and optimization of tube-type receiver panels for molten salt application," *Solar Engineering* 2, pp. 1029–1036, 1992.
8. B. L. Kistler et al., "Fatigue Analysis of a Solar Central Receiver Design Using Measured Weather Data," *Sandia National Laboratories* 1987.
9. A. Bonk, S. Sau, N. Uranga, M. Hernaiz, T. Bauer, "Advanced heat transfer fluids for direct molten salt line-focusing CSP plants," *Progress in Energy and Combustion Science* 67 (2018), pp. 69-87.
10. <http://freegreenius.dlr.de>